IOVS Papers in Press. Published on June 16, 2010 as Manuscript iovs.10-5369

Topography and Tomography Properties of Forme Fruste Keratoconus Corneas.

Alain SAAD MD [1,2]

Damien GATINEL MD, PhD [1,2]

1. Rothschild Foundation, 25 rue Manin, 75019 Paris, France (33-1 48 03 64 86 Fax: 33-1 48 03 64 87)
2. Center for Expertise and Research in Optics for Clinicians (CEROC).

Address for correspondence:

Dr Damien Gatinel
Fondation Ophtalmologique Adolphe de Rothschild
25, Rue Manin
75019, Paris
France

Word count: 3951

The authors received no financial support for the study and have no financial interest related to the article.

Key words: Keratoconus, Forme Fruste keratoconus, keratoconus suspect, tomography, topography, ectasia post Lasik

Abstract

Purpose: To investigate the efficacy of topography and tomography indices combined in discriminant functions to detect mild ectatic corneas.

Methods: We retrospectively reviewed the data of 143 eyes separated into 3 groups by the Nidek Corneal Navigator System of the OPD scan: normal (operated by Lasik with 2 years follow-up) (N) (n=72), Forme Fruste Keratoconus (N Topography with contralateral KC) (FFKC) (n=40) and KC (n=31). Topography and tomography indices, Corneal Thickness Spatial Profile (CTSP), anterior and posterior curvature spatial profiles were obtained with the Orbscan IIz. Percentage of thickness increase (PTI) from the thinnest point to the periphery and percentage of variation of anterior (PVAK) and posterior curvature were calculated and compared using a Kruskall-Wallis test. The usefulness of these data to discriminate between the three groups was assessed using a Receiver-Operating Characteristic (ROC) curve analysis

Results: Posterior Elevation of the Thinnest Point (TP), all positions of CTSP, PTI for all distances from the TP and PVAK from 5mm to 7mm distance from the TP were significantly different in the FFKC as compared to the N group. The discriminant functions between the FFKC and the N group and between the KC and the N group reached an Area under the ROC curve of 0.98 and 0.99 respectively. PTI indices and Maximum Posterior Central Elevation were the most important contributors to the discriminant function.

Conclusion: Indices generated from corneal thickness and curvature measurements over the entire cornea centered on the TP can identify very mild forms of ectasia undetected by a Placido-based neural network program.

Introduction

There has been a great interest in attempting to preoperatively identify patients at risk for post-LASIK corneal ectasia. It's now known that corneas that share similarities with ectatic corneas (Keratoconus or Pellucid Marginal Corneal Degeneration) are at higher risk for this complication[1-4]. Thus efforts are concentrating on using available specular topography, tomography or biomechanical studies in order to recognize Keratoconus (KC) in its earliest stages[5-12]. KC is a noninflammatory progressive localized thinning and protrusion of the cornea. The progressive nature of the disease makes it easily recognized in its advanced stages. However there's a persistent ambiguity regarding the exact definition of a suspect keratoconus (KCS) cornea and there are no widely accepted criteria to categorize an eye as KCS[13-15]. It's discussed whether the first detectable sign of KC, consequently defining the KCS category, is a localized steepening seen with Placido corneal topography[15-19] or a slight bowing of the posterior corneal surface detected by tomography[9, 14, 20]. Current biomechanical parameters (Corneal Hysteresis and Corneal Resistance Factor) studies showed that KCS corneas differ significantly from normal and KC corneas but the results are of little clinical value until now[5]. An important practical task for clinicians is to improve the sensitivity of their screening methods in order to identify patients with mild manifestations of KC, and prevent iatrogenic keratectasia. Even if only one eye is affected initially, KC is an asymmetric progressive disorder that will ultimately affect both eyes. The reported frequency of unilateral KC among all KC

patients varies depending on the methods used for diagnosis. The estimated prevalence of unilateral KC ranges from 14.3% to 41% in studies where only clinical parameters were considered [21-23]. In more recent studies, the reported frequencies based on computerized videokeratography diagnosis techniques, ranged from 0.5% to 4% [18, 24]. Thus the incidence of "true" unilateral KC is very low and some studies suggested that, if patients are observed for a sufficient period of time, signs of keratoconus will develop in the opposite eye[23, 24]. This results from the fact that both eyes of unilateral KC have the same genetic makeup, and therefore the less affected eye is also known to have KC[15], considering that KC is genetically described as a model of autosomal dominant transmission with complete penetrance but incomplete expression[25-28]. Therefore, the term Forme Fruste KC (FFKC) first proposed by Amsler in 1961[29] and then adopted by Klyce, should be used to define the contralateral eye of a unilateral KC), the Forme Fruste being "an incomplete, abortive, or unusual form of a syndrome or disease"[15, 29].

Thus, investigating these particular eyes and finding topographic and tomographic characteristics of these corneas help providing some evidence of what an "at risk" cornea would be.

The aims of our study were to describe and compare topography and tomography indices, as well as the central to periphery percentage of thickness increase and percentage of anterior and posterior curvature modification between 3 groups of corneas classified as Normal (and operated by Lasik with 2 years follow-up), FFKC, and KC by specular topography based on the Nidek

Corneal Navigator artificial intelligence[30-32] and then to combine those indices in discriminant functions in order to detect mild ectatic corneas.

Patients and methods

This retrospective study followed the tenets of the declaration of Helsinki and included 143 eyes of 143 patients that were divided into 3 groups: normal, FFKC and KC. Only one eye was included for each patient.

The Orbscan IIz (Bausch & Lomb Surgical, Rochester, NY) and OPD-Scan (Nidek CO., LTD, Gamagori, Japan) videokeratographs were obtained by 2 experienced operators. Segregation of the three groups was based on the results of the Nidek Corneal Navigator (NCN) that uses an artificial intelligence technique to train a computer neural network to recognize specific classifications of corneal topography. The NCN first calculates various indices representing corneal shape characteristics. The indices are then used by the NCN to score the measurement's similarity to 9 clinical classification types: normal, astigmatism, keratoconus suspect, keratoconus, pellucid marginal degeneration, post-keratoplasty, myopic refractive surgery, hyperopic refractive surgery and unclassified variation. These diagnostic results are estimated based on the relationship between the corneal indices and cases. The percentage of similarity is indicated for each diagnostic condition; the value varies from 0% to 99%. The indicated result for each topography condition is independent from other categories.

Eyes in the normal group had a score of 99% similarity to normality using the NCN analysis. In addition, data provided by the Orbscan IIz for the normal group did not reveal any topography patterns suggestive of KCS such as focal or inferior steepening of the cornea or central keratometry greater than 47.0

diopters (D). This group was composed of 72 eyes operated by Lasik with a two year follow up, where no complications such as ectasia were observed. The FFKC group was composed of 40 contralateral eyes of KC (figures 1 and 2). The NCN analysis indicated a null score similarity to KCS and KC for the selected eyes and a non null score similarity to KC for the contralateral eyes (figure 2). The contralateral eye had also a frank KC aspect on the curvature topography. The keratoconus group included 31 eyes that had frank keratoconus diagnosed by an experienced corneal specialist on the basis of clinical and topographic signs (with a positive similarity score to KC indicated by the NCN).

Orbscan IIz is a 3-dimensional slit-scanning topography system for analysis of the corneal anterior and posterior surfaces as well as pachymetry. It uses a slit-scanning system to measure 18000 data points and uses a Placido-based system to make necessary adjustments to produce topography data.

On the Orbscan IIz, elevation maps are by default plotted against a spherical reference surface whose radius and position are calculated without constraints (float mode). The following criteria were analyzed and compared using the Orbscan quad map representation: central power and radius in both anterior Best Fit Sphere (BFS) and posterior BFS; Maximum Anterior Central Elevation (MACE) and Posterior Central Elevation value (MPCE) relative to the BFS in the central 1.0 mm radius zone; simulated keratometry in maximum (SKmax) and minimum (SKmin) dioptric values; irregularity index at 3.0 mm and at 5.0 mm; central pachymetry (CP); thinnest pachymetry (TP); magnitude of the Decentration of the Thinnest corneal Point from the corneal geometric center

(DTP). All values except MACE and MPCE are directly available from the ‘‘Quad Map display’’ mode. The MACE and MPCE values can be obtained via the ‘‘Stats’’ menu, which is accessed through the ‘‘Tools’’ menu on the main toolbar. The elevation, topography and tomography maps can be rotated to view the acquired image in a different perspective. This is accomplished by determining the perpendicular to the surface at the specified center location. The surface is then rotated to bring the new center to the map center and the surface normal parallel to the instrument axis. This can be obtained via the ‘‘tools’’ menu, by clicking on the surface rotation button and selecting the preferred center location. We considered the thinnest point of the cornea as the center location to obtain the following data:

- The elevation of the thinnest point (AETP and PETP: Anterior and Posterior Elevation of the Thinnest Point). They were acquired by manually guiding the cursor over the center of the anterior and posterior elevation maps, respectively.

-The anterior and posterior averages of keratometry values of the points on 9 circular adjacent rings of 0.5mm width centered on the thinnest point. These keratometry values were processed from the slit scanning data rotated and centered on the TP. The outer diameter of each ring varied from 1 mm (inner ring) to 9 mm (outer ring). Knowing the mean keratometry of each ring, we calculated the anterior and posterior central to periphery Percentage of Variation in Anterior and Posterior curvature (Increase or Decrease) ($PVAK_{n,}$ and $PVPK_n$) for each radius using the formula: $PVA(P)K_n = (K_n - (K_{n-0.5}))/K_{n-0.5}$ where Kn is the mean corneal curvature at each radius and n represents the radius of imaginary

rings centered on the thinnest point. In contrast to Asphericity which is a global descriptor of the rate of change of curvature between the centre and the periphery of the cornea, the PVA(P)K represent the local variation in the curvature with step of 0.5mm of radius. Therefore, it provides a more exhaustive and complete approach to investigate the changes in corneal curvature in the studied population. Similarly, the averages of thickness values of the points located on 9 rings centered on the thinnest point were obtained to create the corneal thickness profile. We calculated the Percentage of Thickness Increase[33, 34] for each ring (PTI) using the following formula: $PTI = (T_n - TP)/TP$ where Tn is the corneal thickness average at each rings and n represents the radius of the outer perimeter of each ring centered on the thinnest point (TP).

All numerical results were entered into a database, and statistical analyses were performed with XLSTAT2009 (Addinsoft) using the Kruskall-Wallis test followed by a Dunn procedure for multiple non parametric comparisons and a Bonferroni correction to maintain a global level of $p<0.05$.

Discriminant analysis was used to determine the group of an observation based on a set of variables obtained from the anterior and posterior corneal surface and from thickness spatial profile. Based on the N and FFKC group, the discriminant analysis constructs a set of linear functions of the variables, known as discriminant functions, such as

$L = b_1x_1 + b_2x_2 + b_nx_n + c$, where the b's are discriminant coefficients, the x's are the input variables and c is a constant. The following discriminant functions were generated:

FT: Elevation and decentration of the TP

FPTI: Percentage of Thickness Increase over the entire cornea

FPVAK: Percentage of Variation of Anterior Curvature over the entire cornea

FPVPK: Percentage of Variation of Posterior Curvature over the entire cornea

FI: Irregularity at 3 and 5 mm

FA: All the studied indices

The discriminant functions can be used to predict the class of a new observation with unknown class.

Receiver operating characteristic (ROC) curves were plotted to obtain critical values that allow classification with maximum accuracy. For the output values of the discriminant functions tested, the area under the ROC curve, sensitivity (true positive/ (true positive+false negative)), specificity (true negative/ (true negative+false positive)) accuracy ((true positive+true negative)/ total number of cases), and cutoff value were calculated.

Results

Table 1 compares demographic data between the 3 groups. There were significantly more males in the KC and the FFKC group ($p<0.001$). The mean age was not statistically different between the groups. Table 2 represents the mean and standard deviation of the studied factors as well as an inter-group comparison.

Normal and FFKC groups:

There was no significant difference between the normal group and the FFKC group for the ABFS, PBFS, SK max and SK min. The 3 mm and 5 mm irregularities were significantly higher in the FFKC group. The CP was significantly lower in the FFKC group compared to the normal group and the TP was significantly thinner and decentered. The difference between the CP and the TP (CP- TP) and the PETP values were significantly higher in the FFKC group compared to the normal group (table 2) The MACE, MPCE and AETP were not significantly different between the 2 groups..

Normal and KC groups:

The anterior and posterior elevation indices deriving from the quad map (ABFS, PBFS, SK max and SK min, irregularity at 3mm and 5mm) were significantly different in the KC group as compared to the Normal group. The CP and the TP were also significantly different in the 2 groups and the difference between the

CP and the TP (CP – TP) was significantly higher in the KC group. The TP was more infero-temporally located in the KC group compared to the normal group and the MACE, MPCE, AETP and PETP were significantly higher in the KC group (table 2).

Anterior corneal curvature:

The mean anterior curvature was significantly different for any distance from the cornea's thinnest point except at 8.0 and 9.0 mm between the normal group and the KC group but not between the normal group and the FFKC group (table 2 and figure 3). The cornea flattened significantly faster at 5.0 mm, 6.0 mm and 7.0 mm from the thinnest point in the FFKC group compared to the normal group (figure 4).

Corneal thickness spatial profile:

The mean thickness of all corneal zones was significantly lower in the FFKC and KC group compared to the normal group (table 2 and figure 5). The cornea thickened significantly faster from the thinnest point to the periphery for all corneal zones in the FFKC and KC group compared to the normal group (figure 6).

Posterior corneal curvature:

The mean posterior curvature was significantly lower from 1mm to 6mm distance from the cornea's thinnest point between the normal group and the KC group but

not between the normal group and the FFKC group (table 2). The cornea flattened significantly faster from 3.0 mm to 9.0 mm from the thinnest point in the KC group compared to the normal group (table 2).

Discriminant analysis and ROC curve

The formulas of all discriminant functions are shown in the appendix. The functions were derived from N and FFKC indices and their output values were tested to differentiate between N and FFKC group and N and KC group. The output values of the discriminant function were significantly different between the three groups ($p<0.0001$) (table 3).

The function FT consisted of the TP, the difference between CP and TP, the Decentration of the TP and the AETP and PETP where the difference between CP and TP had the highest discriminant coefficient (0.501).

The function FPTI consisted of the PTI over the entire cornea where the PTI at 4mm from the TP had the highest discriminant coefficient (2.846).

The function FPVAK consisted of the PVAK over the entire cornea where the PVAK at 5mm from the TP had the highest discriminant coefficient (1.019).

The function FPVPK consisted of the PVPK over the entire cornea where the PVPK at 2mm from the TP had the highest discriminant coefficient (0.527).

The function FI consisted of the irregularity at 3 and 5mm, where the irregularity at 5 mm had the highest discriminant coefficient (0.543).

The function FA was derived from all the studied factors. The percentage of thickness increase (PTI) at 5mm and 6mm from the TP had the highest relative

discriminant coefficient (6.555 and 5.826) followed by the PTI at 3mm (3.117), 8mm (1.497), 2mm (1.473), the MPCE (1.384), the PVAK at 5mm (1.203), and the PVPK at 4mm (1.040). Others indices had a relative discriminant coefficient less than 1.

For the distinction between the N group and the FFKC, the FA based on all the studied indices reached an area under the ROC curve (AUROC) of 0.98, a sensitivity of 93%, a specificity of 92% and an accuracy of 92% (table 4). The other functions had an accuracy between 71% (FPVAK) and 76% (FT).

For the distinction between the N group and the KC group, all the output values of the discriminant functions yielded a sensitivity and a specificity higher than 90% except the FPVPK (87% for both), with the FI reaching the same accuracy as FA (99%) (Table 4). The FA could differentiate the KC group from the N group with an AUROC of 0.99, a sensitivity of 97%, a specificity of 100% and an accuracy of 99%. In figure 7 and 8 the ROC curves of all the discriminant functions are displayed graphically.

Discussion

To describe the characteristics of the earliest form of KC and avoid any biases in the training sample, objective selection of patients in each studied group is crucial. For that purpose, the artificial intelligence of the NCN is preponderant and, while others studied clinically unilateral KC[8, 23, 35], it's the first study to our knowledge, to describe characteristics of FFKC selected using neural network criteria: a positive percentage of similarity to normal eyes on the NCN with a null percentage of similarity to KC and KCS. KC is defined as a condition in which the cornea assumes a conical shape because of thinning and protrusion[22]. We recently described a case of bilateral post femtosecond LASIK ectasia occurring in topographically normal eyes presenting only a 20 microns difference in CP and in TP between both eyes[36] and Li Lim and al[35] and Pflugfelder and al[37] already showed that corneal thinning is a key pathologic feature of KC. Thus studying the characteristics of the cornea centered on the thinnest point, which corresponds to the most affected point, can be of valuable interest and the preliminary work of Ambrosio and al[33] showed consistent results and proved that the percentage of thickness increase from the TP to the periphery is different in keratoconic eyes compared to normal eyes. Our results went further and provided evidence that the PTI in the mildest manifestations of the keratoconus disease (FFKC) is already higher compared to normal eyes (figures 6). The PVAK was also significantly different at 5.0mm, 6.0 mm and 7.0 mm distance from the TP between normal eyes and FFKC eyes (figure 4). These results strongly suggest

that the mildest form of KC is characterized by a quickest modification of the cornea's shape and thickness from the thinnest point to the periphery.

There was no significant difference in the ABFS, PBFS, SK max and SK min between normal eyes and FFKC (table 2) which reflected the null similarity to KCS found on the NCN. One of the first detectable sign of keratoconus with Placido corneal topography is a localized steepening [15]. The FFKC is a mildest stage of the disease; the eyes included in our FFKC group were negative for KC and KCS detection based on anterior curvature data only. Thus current Placido based indices were not sensitive enough to detect the earliest forms of KC. Irregularity indices at 3 mm and 5 mm show the optical surface irregularity that is proportional to the standard deviation of the axis-independent surface curvature. They are calculated automatically from within the Orbscan IIz software according to a statistical combination of the standard deviations of the mean and toric curvatures [38]. Some authors reported that these irregularity indices were significantly higher in KCS corneas compared to normal corneas [35, 39]. Interestingly, in our study the 3 and 5 mm irregularity indices were significantly higher in FFKC compared to Normal corneas; however this level of irregularity was not sufficient to exceed the threshold for positive KCS suspicion with the NCN. The CP and the TP were significantly lower in FFKC ($p<0.0001$, table 2) and the subtraction between the CP and the TP (CP-TP) significantly differentiated the 3 groups (table 2). It was previously reported that the TP of keratoconic eyes is typically located inferotemporally [40, 41]. We found that the thinnest point of FFKC was located inferiorly compared to the normal eyes ($p <$

0.0001, table 2). Horizontal and vertical displacement of the thinnest point on the pachymetry map is commonly associated with poor patient fixation or operator centration during acquisition of the Orbscan IIz image [6]. However multiple Orbscan images were acquired for our FFKC groups. Many studies described modifications in the posterior corneal surface in keratoconus[14, 35, 42] and some authors proposed a KC screening algorithm using the posterior elevation on Orbscan IIz combined with videokeratography[9].The PETP was significantly higher in FFKC ($p<0.0001$, table 2) compared to normal corneas. Thus, even if not identified as suspect by Placido topography indices, the FFKC group had PETP significantly higher than normal corneas. This result corroborates the hypothesis that an increase in posterior elevation concomitant to paracentral corneal thinning may be the first sign of subclinical keratoconus [9, 14].

Tomidokoro et al[43] already showed that the central posterior corneal curvature was significantly lower (larger absolute value) in KCS and KC eyes compared to Normal eyes and concluded that deformation, including local protrusion, occurs not only in the anterior but also in the posterior corneal surface of keratoconus eyes. We found a significantly larger absolute value for posterior curvature from 1.0 mm to 6.0 mm distance from the thinnest point in KC eyes compared to N eyes however the difference was not statistically different between the Normal group and the FFKC group. The percentage of variation of the posterior curvature (PVPK) from the thinnest point was not significantly different between N group and FFKC group. Thus elevation indices of the posterior surface (MPCE,

PETP) seem to be more sensitive than posterior curvature indices in discriminating between Normal eyes and mild KC eyes.

As shown in table 4, the majority of the discriminant functions were able to separate between the N group and the KC group which supports the idea that frank keratoconus is an easily detectable entity.

Furthermore, combining the anterior surface irregularity indices only provides a highly accurate tool in detecting KC (FI: sensitivity: 100%, specificity: 99%, Accuracy: 99%). This accuracy reached the one obtained with the association of all the studied factors (FA: sensitivity: 97%, specificity: 100%, Accuracy: 99%). However, all the functions that combine indices of the same origin (Irregularity alone, Thinnest point related indices alone, Thickness Spatial Profile alone or Curvature alone) (FI, FT, FPTI, FPVAK and FPVPK) could not be accurate enough in separating the N group from the FFKC group (Accuracy between 71% and 76%). Only the combination of all the studied indices in a discriminant function (FA) allowed the differentiation between the N group and the FFKC with a good accuracy (92%) (Sensitivity: 92.5% and specificity 92%). As the reported frequencies of unilateral KC range between 0.5% and 4%, cases of true unilateral KC may rarely occur, probably due to an intense trauma or severe eye rubbing. This may explain the sensitivity of 92.5 % found in differentiating between N group and FFKC group, the undetected cases (3 false negative) may be “true” unilateral KC. Using the same function, differentiation between N group and KC group is possible with a sensitivity of 97% and a specificity of 100% (Table 4). Discriminant functions are interpreted by means of standardized

coefficients. The larger the standardized coefficient, the greater is the contribution of the respective variable to the discrimination between groups. Spatial thickness profile indices and MPCE were the most important contributors to FA.

This study showed that indices generated from corneal thickness and curvature measurements over the entire cornea and calculations of percentage of thickness increase and percentage of anterior and posterior curvature variation from the thinnest point to the periphery can identify very mild forms of KC undetected by Placido topography. However, we cannot conclude that any single parameter taken alone is sufficient to distinguish a normal from a suspicious cornea as the studied indices values showed some degree of overlap in normal and pathologic corneas. A retrospective study of all the reported indices in “unsolved” ectasia cases (without known risk factors as KCS aspect or residual stromal bed of less than 300 microns) could confirm the link between our findings and the risk of ectasia. Additionally, it could not be ruled out that there are other entities at risk for iatrogenic ectasia that could not be detected by our approach.

Currently, most diagnostic and classification criteria for keratoconus are based on anterior corneal curvature data [19, 32, 44] and do not take into account the spatial thickness profile and other corneal indices provided by tomography. We believe that evaluating those indices in conjunction with the parameters provided by Placido topography may help in creating artificial intelligence more sensitive and specific for the detection of corneas at risk for refractive surgery. Considering our results, new charts and graphs exploring data derived from elevation and

pachymetry maps should be generalized in future corneal topography's software in order to help the clinician detecting mild form of ectasia.

Appendix

Relative coefficients of the discriminant function indices:

FT = 0.412 x TP -0.501 x (CP-TP) – 0.188 x DTP -0.362 x AETP + 0.220 x PETP

FPTI = -0.062 x PTI2 -1.468 x PTI3 + 2.846 x PTI4 +1.436 x PTI5 -1.0 x PTI6 – 1.203 x PTI7 -0.868 x PTI8 + 1.219 x PTI9

FPVAK = -0.027 x PVAK2 +0.463 x PVAK3 -0.824 x PVAK4 + 0.522 x PVAK5 - 1.019 x PVAK6 + 0.013 x PVAK7 -0.075 x PVAK8 + 0.236 x PVAK9

FPVPK = 0.527 x PVPK2 -0.195 x PVPK3 +0.016 x PVPK4 -0.518 x PVPK5 - 0.258 x PVPK6 + 0.090 x PVPK7 + 0.482 x PVPK8 + 0.029 x PVPK9

FI = 0.322 x (Irreg 3mm) + 0.543 x (Irreg 5 mm)

FA = 0.174 x (Irreg 3mm) + 0.151 x (Irreg 5mm) - 0.180 x (TP) +0.065 x (CP - TP) -0.685 x dec lyl +0.547 x (DTP) - 0.780 x (MACE) +1.384 x (MPCE) +0.635 x (AETP) - 0.782 x (PETP) +1.473 x (PTI2) -3.117 x (PTI3) +0.841 x (PTI4) +6.555 x (PTI5) - 5.826 x (PTI6) - 1.198 x (PTI7) + 1.497 x (PTI8) +0.179 x (PTI9) + 0.433 x (PVAK2) -0.349 x (PVAK3) – 0.854 x (PVAK4) +1.203 x (PVAK5) - 0.979 x (PVAK6) +0.250 x (PVAK7) +0.324 x (PVAK8) + 0.217 x (PVAK9) + 0.650 x (PVPK2) - 0.290 x (PVPK3) +1.040 x (PVPK4) -0.736 x (PVPK5) +0.604 x (PVPK6) + 0.449 x (PVPK7) + 0.522 x (PVPK8) - 0.340 x (PVPK9)

FIGURES

Characteristics	Normal	FFKC	KC
Patients (n)	72	40	31
OD n (%)	44 (61)	20 (50)	16 (52)
Mean age (y) +/- SD	33.3 +/- 9.3	33.4 +/- 13.1	32.0 +/- 7.7
Male sex, n (%)	24 (33)	27 (67)	24 (77)
SE (D) mean, (Range)	-4.16 ± 2.77 (-11.00 ; -0.50)	-1.13 +/- 0.96 (-2.50 ; 0.50)	-7.74 +/- 3.14 (-15.75 ; 0.00)

Table 1: Demographic characteristics of patients
SE: Spherical Equivalent

	Mean and SD			Kruskal-Wallis and Dunn Procedure		
	N	FFKC	KC	N vs FFKC	N vs KC	KC vs FFKC
n	72	40	31			
Anterior BFS (D)	42.5 +/- 1.1	42.24 +/- 1.44	43.64 +/- 1.77	>0.05	0.001	0.001
Posterior BFS (D)	51.6 +/- 1.8	51.36 +/- 2.26	54.01 +/- 2.74	>0.05	< 0.0001	< 0.0001
Max Sim K (D)	43.9 +/- 1.2	43.69 +/- 1.60	48.37 +/- 4.20	>0.05	< 0.0001	< 0.0001
Min Sim K (D)	43.1 +/- 1.2	42.8 +/- 1.6	45.2 +/- 3.4	>0.05	0.002	0.002
Irreg 3mm (D)	0.98 +/- 0.34	1.25 +/- 0.38	5.01 +/- 2.47	< 0.0001	< 0.0001	< 0.0001
Irreg 5mm (D)	1.3 +/- 0.3	1.64 +/- 0.42	4.98 +/- 2.35	< 0.0001	< 0.0001	< 0.0001
Central Pachymetry (microns)	554.6 +/- 36.1	524.3 +/- 37.0	487.5 +/- 52.1	< 0.0001	< 0.0001	< 0.0001
Thinnest pachymetry (microns)	547.8 +/- 36.3	512.2 +/- 37.6	464.2 +/- 55.0	< 0.0001	< 0.0001	< 0.0001
Difference CP - TP	6.8 +/- 3.1	12.1 +/- 5.6	23.3 +/- 14.3	< 0.0001	< 0.0001	< 0.0001
Decentration TP x	0.33 +/- 0.47	0.49 +/- 0.59	0.67 +/- 0.31	> 0.05	0.002	> 0.05
Decentration TP y	"-0.22 +/- 0.36	"-0.47 +/- 0.50	"-0.51 +/- 0.47	< 0.001	< 0.001	> 0.05
Decentration TP ($\sqrt{((TPx)^2+(TPy)^2}$)	0.64 +/- 0.32	0.95 +/- 0.37	0.96 +/- 0.30	< 0.0001	< 0.0001	> 0.05
MACE	10.6 +/- 3.6	12.6 +/- 4.2	42.1 +/- 21.2	> 0.05	< 0.0001	< 0.0001
MPCE	21.9 +/- 7.9	27.2 +/- 11.2	79.0 +/- 38.8	> 0.05	< 0.0001	< 0.0001
AETP	7.4 +/- 3.5	9.3 +/- 3.8	33.0 +/- 23.5	> 0.05	< 0.0001	< 0.0001
PETP	19.7 +/- 8.6	26.3+/- 11.0	73.2 +/- 37.5	< 0.0001	< 0.0001	< 0.0001
Ant curvature						
1 mm	43.29 +/- 1.47	43.47 +/- 1.55	50.46 +/- 6.40	> 0.05	< 0.0001	< 0.0001
2 mm	43.36 +/- 1.36	43.52 +/- 1.46	50.13 +/- 5.82	> 0.05	< 0.0001	< 0.0001
3 mm	43.44 +/- 1.23	43.53 +/- 1.36	49.13 +/- 4.72	> 0.05	< 0.0001	< 0.0001
4 mm	43.43 +/- 1.19	43.43 +/- 1.36	47.73 +/- 3.70	> 0.05	< 0.0001	< 0.0001
5 mm	43.32 +/- 1.18	43.24 +/- 1.39	46.26 +/- 2.90	> 0.05	< 0.0001	< 0.0001
6 mm	43.14 +/- 1.16	42.96 +/- 1.39	44.99 +/- 2.32	> 0.05	< 0.0001	< 0.0001
7 mm	42.84 +/- 1.13	42.58 +/- 1.39	43.98 +/- 1.93	> 0.05	0.002	0.002
8 mm	42.46 +/- 1.07	42.17 +/- 1.39	43.17 +/- 1.75	> 0.05	> 0.05	0.014
9 mm	42.00 +/- 1.05	41.72 +/- 1.48	42.49 +/- 1.57	> 0.05	> 0.05	0.032
Pachymetry						
1 mm	0.549 +/- 0.036	0.515 +/- 0.035	0.467 +/- 0.054	< 0.0001	< 0.0001	< 0.0001
2 mm	0.554 +/- 0.036	0.520 +/- 0.035	0.476 +/- 0.053	< 0.0001	< 0.0001	< 0.0001
3 mm	0.563 +/- 0.035	0.531 +/- 0.035	0.494 +/- 0.050	< 0.0001	< 0.0001	< 0.0001
4 mm	0.575 +/- 0.035	0.546 +/- 0.034	0.518 +/- 0.048	< 0.0001	< 0.0001	> 0.05
5 mm	0.591 +/- 0.035	0.563 +/- 0.034	0.546 +/- 0.046	< 0.0001	< 0.0001	> 0.05
6 mm	0.611 +/- 0.035	0.583 +/- 0.034	0.575 +/- 0.044	< 0.0001	< 0.0001	> 0.05
7 mm	0.632 +/- 0.036	0.604 +/- 0.035	0.602 +/- 0.041	< 0.0001	< 0.0001	> 0.05
8 mm	0.656 +/- 0.038	0.627 +/- 0.036	0.628 +/- 0.040	< 0.0001	< 0.0001	> 0.05
9 mm	0.673 +/- 0.040	0.646 +/- 0.038	0.646 +/- 0.039	< 0.0001	< 0.0001	> 0.05
Posterior curvature						
1 mm	"-6.17 +/- 0.46	"-6.05 +/- 0.78	"-7.69 +/- 1.23	> 0.05	< 0.0001	< 0.0001
2 mm	"-6.50 +/- 0.25	"-6.64 +/- 0.39	"-8.22 +/- 1.10	> 0.05	< 0.0001	< 0.0001
3 mm	"-6.44 +/- 0.23	"-6.54 +/- 0.33	"-7.83 +/- 0.89	> 0.05	< 0.0001	< 0.0001
4 mm	"-6.38 +/- 0.22	"-6.43 +/- 0.29	"-7.39 +/- 0.67	> 0.05	< 0.0001	< 0.0001
5 mm	"-6.32 +/- 0.21	"-6.32 +/- 0.26	"-6.96 +/- 0.49	> 0.05	< 0.0001	< 0.0001
6 mm	"-6.23 +/- 0.21	"-6.20 +/- 0.26	"-6.58 +/- 0.36	> 0.05	< 0.0001	< 0.0001
7 mm	"-6.13 +/- 0.22	"-6.10 +/- 0.29	"-6.27 +/- 0.32	> 0.05	> 0.05	> 0.05
8 mm	"-6.03 +/- 0.24	"-6.04 +/- 0.36	"-6.07 +/- 0.31	> 0.05	> 0.05	> 0.05
9 mm	"-5.92 +/- 0.25	"-5.92 +/- 0.37	"-5.95 +/- 0.37	> 0.05	> 0.05	> 0.05
Percentage of variation of posterior curvature						

2 mm	6.00 +/- 10.76	11.28+/- 13.35	7.96 +/- 12.88	> 0.05	> 0.05	> 0.05
3 mm	"-0.88 +/- 1.39	"-1.52 +/- 1.87	"-4.45 +/- 2.66	> 0.05	0.032	< 0.05
4 mm	"-0.90 +/- 1.02	"-1.61 +/- 1.61	"-5.39 +/- 2.79	> 0.05	< 0.001	< 0.001
5 mm	"-1.06 +/- 0.88	"-1.73 +/- 1.31	"-5.57 +/- 2.88	> 0.05	< 0.0001	< 0.0001
6 mm	"-1.33 +/- 0.94	"-1.88 +/- 1.02	"-5.32 +/- 2.88	> 0.05	< 0.0001	< 0.0001
7 mm	"-1.56 +/- 1.11	"-1.55 +/- 1.99	"-4.64 +/- 2.73	> 0.05	< 0.0001	< 0.0001
8 mm	"-1.66 +/- 1.00	"-1.06 +/- 2.21	"-3.19 +/- 2.45	> 0.05	< 0.0001	< 0.0001
9 mm	"-1.85 +/- 1.81	"-1.91 +/- 2.74	"-2.00 +/- 2.62	> 0.05	< 0.0001	< 0.0001

Table 2: Mean and standard deviation of the entire studied factors and intergroup comparison.

	N	FFKC	KC
FA (Mean +/- SD) **Range**	0.55 +/- 0.78 -0.67 ; 2.28	3.55 +/- 1.32 1.66 ; 6.33	14.73 +/- 8.60 2.14 ; 31.99
FT	7.04 +/- 0.77 5.44 ; 8.37	5.35 +/- 1.31 1.76 ; 7.72	1.35 +/- 3.27 -5.45 ; 7.43
FPTI	2.88 +/- 0.91 0.54 ; 4.94	3.99 +/- 1.13 2.056 ; 7.45	7.65 +/- 3.47 1.89 ; 16.19
FPVAK	1.89 +/- 0.82 -0.31 ; 3.64	2.35 +/- 1.26 -0.25 ; 5.20	10.30 +/- 7.55 -10.64 ; 25.62
FPVPK	0.57 +/- 0.91 -1.49 ; 4.37	1.63 +/- 1.13 -0.28 ; 4.05	3.70 +/- 2.45 -0.40 ; 10.34
FI	3.72 +/- 0.89 2.37 ; 7.00	4.76 +/- 1.16 3.22 ; 8.26	15.13 +/- 7.16 6.25 ; 29.00

Table 3: Mean, Standard deviation, and range of the output values of the discriminant functions ($p < 0.001$ between the 3 groups).

Discriminant Function	Cut Off value		AUROC		Sensitivity (%)		Specificity (%)		Accuracy (%)	
	N vs FFKC	N vs KC	N vs FFKC	N vs KC	N vs FFKC	N vs KC	N vs FFKC	N vs KC	N vs FFKC	N vs KC
FA	≥ 1.55	≥ 2.69	0.98	0.99	93	97	92	100	92	99
FT	≤ 6.66	≤ 5.71	0.86	0.97	85	93	71	93	76	93
FPTI	≥ 3.38	≥ 4.18	0.77	0.93	70	90	72	93	72	92
FPVAK	≥ 1.75	≥ 3.36	0.74	0.94	70	90	71	97	71	95
FPVPK	≥ 0.88	≥ 1.31	0.78	0.91	72	87	71	87	72	87
FI	≥ 4.13	≥ 6.25	0.78	0.99	72	100	71	99	72	99

Table 4: Cut Off values, Area Under the ROC curve (AUROC), Sensitivity, Specificity and Accuracy of the output values of the discriminant functions.

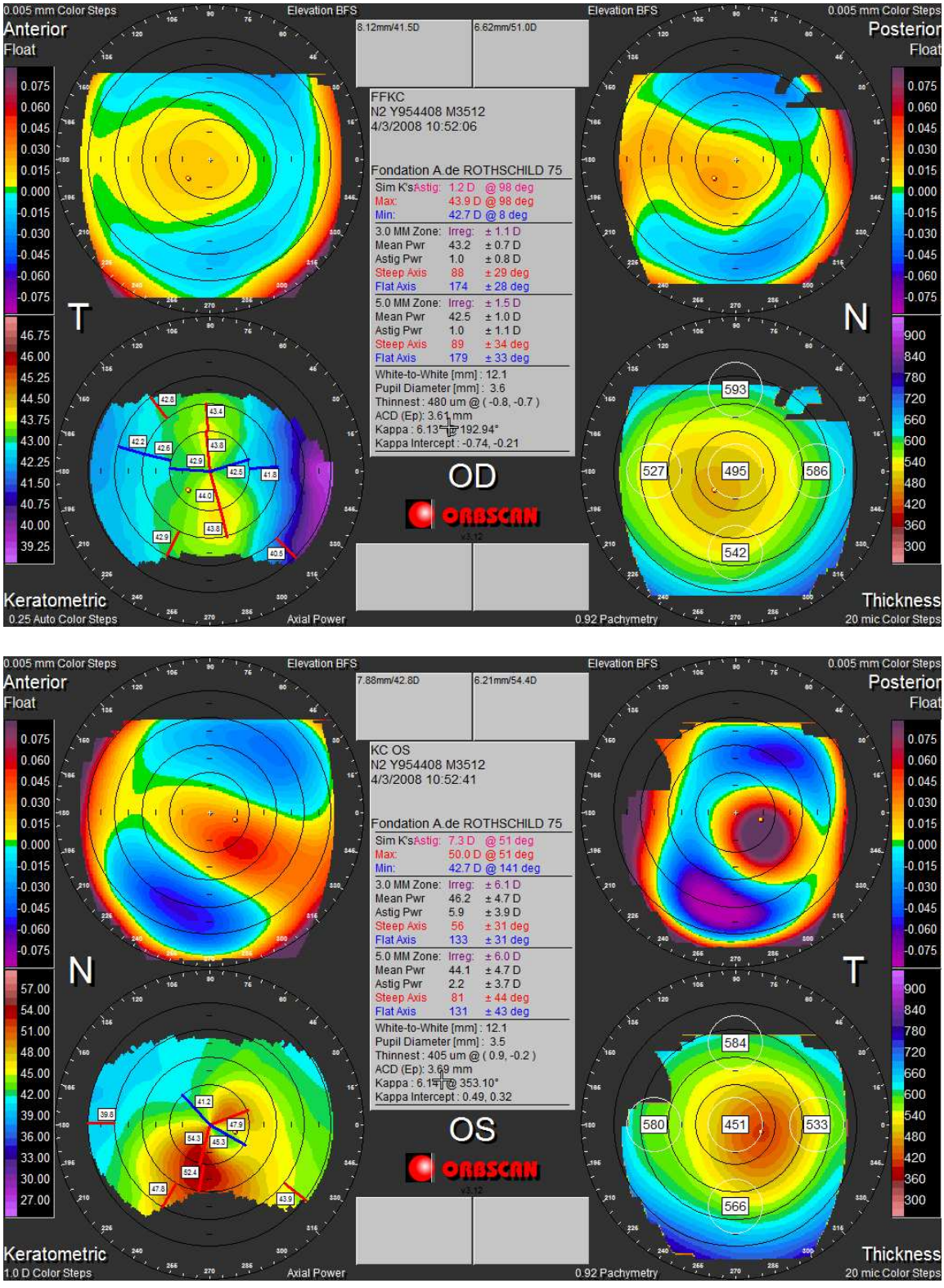

Figure 1: Orbscan IIz quad map of a FFKC (OD) and the contralateral KC (OS)

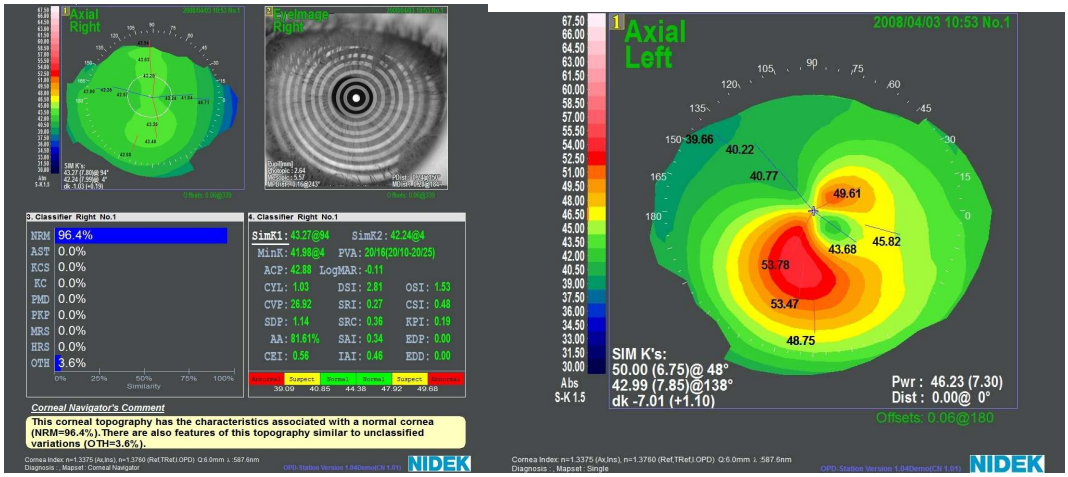

Figure 2: OPD scan and NCN of the FFKC (OD) eye described in figure 1and the contralateral KC.

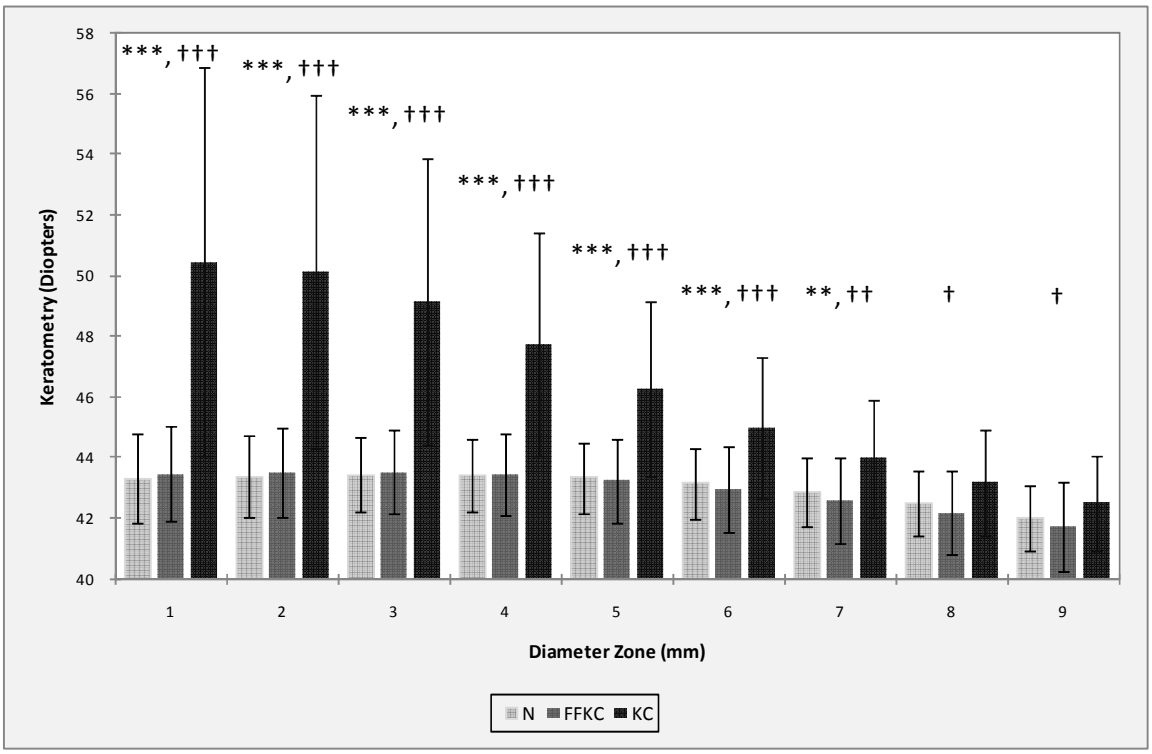

Figure 3 :Mean corneal curvature values on ring concentrically to the thinnest point.
***: p<0.0001 between N and KC groups
**: p<0.001 between N and KC groups
†††: p<0.0001 between FFKC and KC groups
††: p<0.001 between FFKC and KC groups
†: p<0.05 between FFKC and KC groups

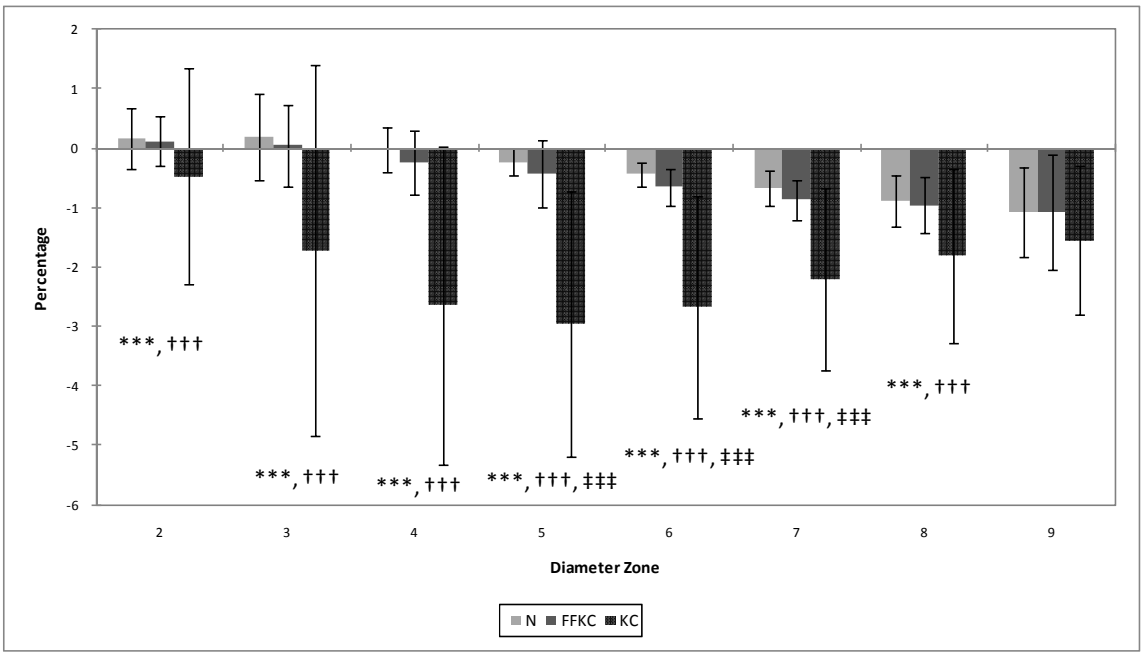

Figure 4 : Percentage of variation of anterior curvature from the thinnest point to the periphery.
***: p<0.0001 between N and KC groups
†††: p<0.0001 between FFKC and KC groups
‡‡‡: p<0.0001 between N and FFKC groups

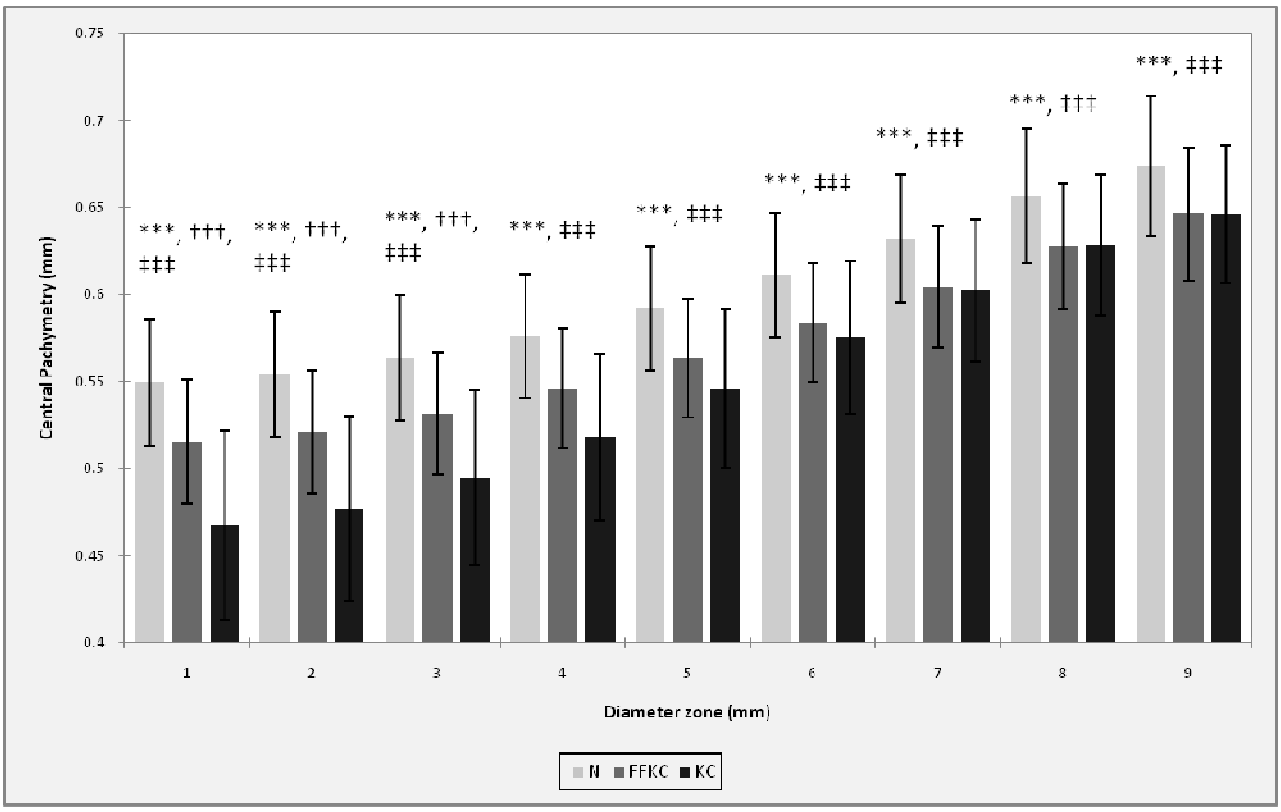

Figure 5: Mean corneal thickness values on rings concentrically to the thinnest point.
***: p<0.0001 between N and KC groups
†††: p<0.0001 between FFKC and KC groups
‡‡‡: p<0.0001 between N and FFKC groups

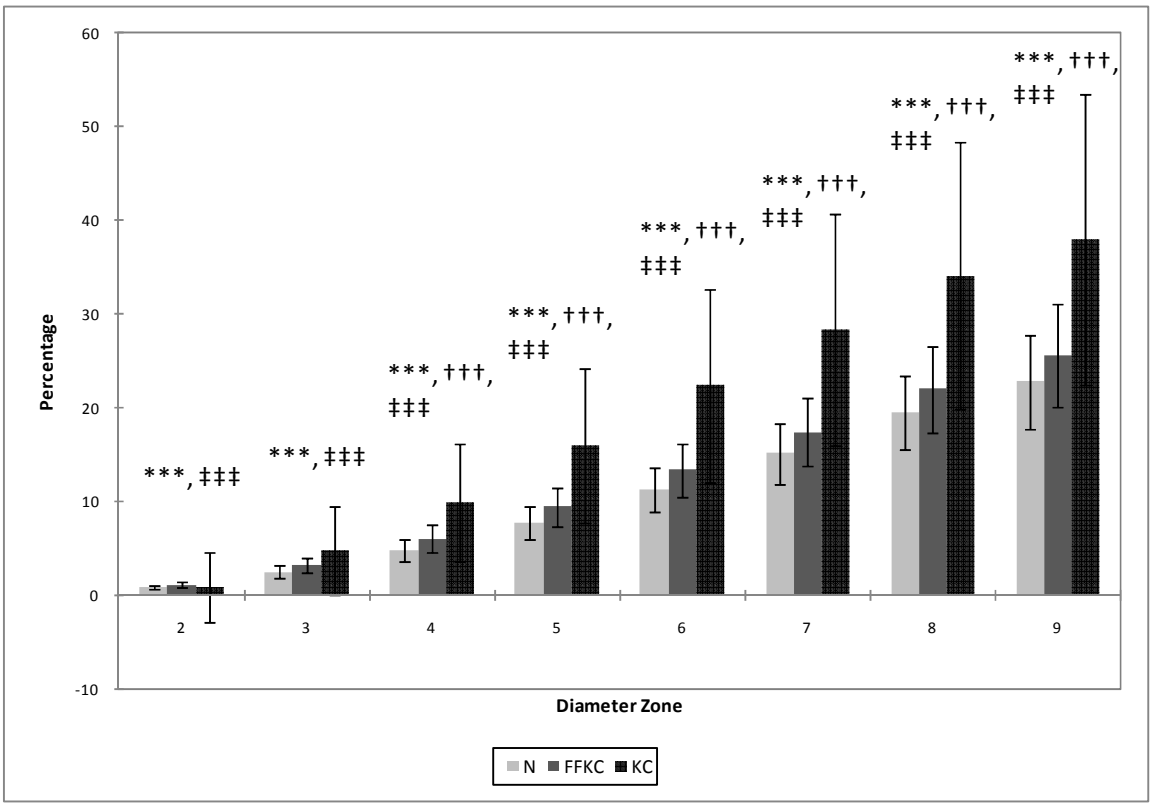

Figure 6: Percentage increase in thickness from the thinnest point to the periphery.
***: p<0.0001 between N and KC groups
†††: p<0.0001 between FFKC and KC groups
‡‡‡: p<0.0001 between N and FFKC groups

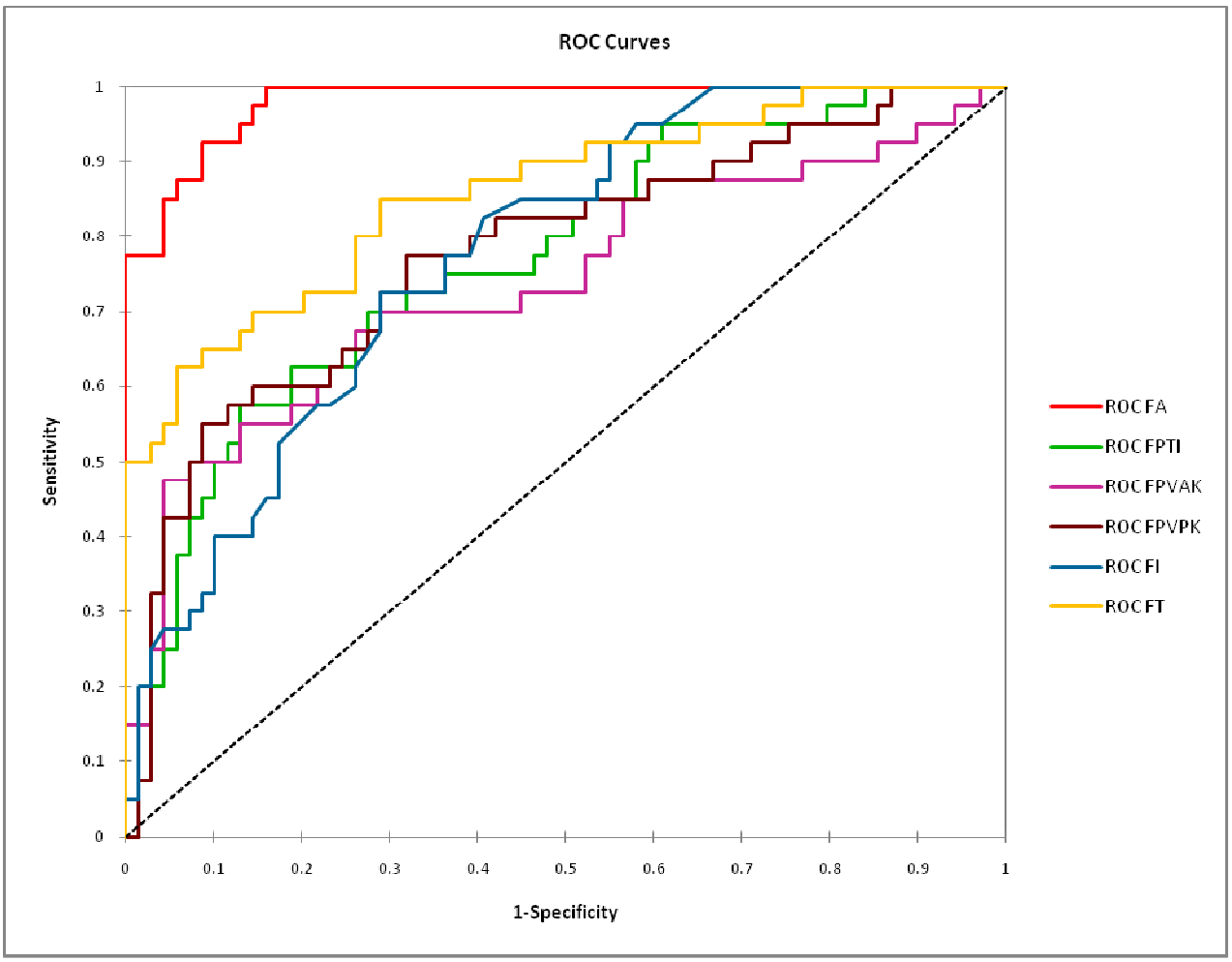

Figure 7: Receiving Operating Characteristic curves of the different functions for discrimination between N group and FFKC group.

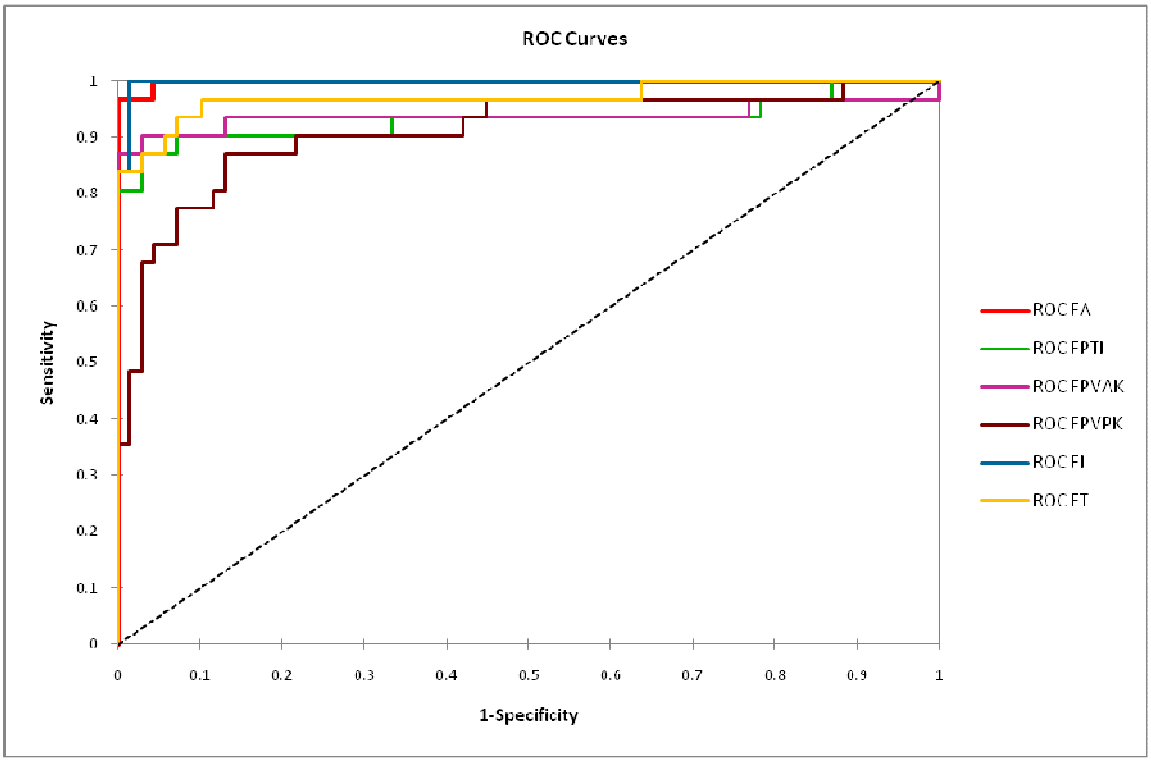

Figure 8: Receiving Operating Characteristic curves of the different functions for discrimination between N group and KC group.

References

1. Binder PS. Analysis of ectasia after laser in situ keratomileusis: risk factors. *J Cataract Refract Surg* 2007;33:1530-1538.
2. Binder PS. Risk factors for ectasia after LASIK. *J Cataract Refract Surg* 2008;34:2010-2011.
3. Randleman JB, Trattler WB, Stulting RD. Validation of the Ectasia Risk Score System for preoperative laser in situ keratomileusis screening. *Am J Ophthalmol* 2008;145:813-818.
4. Randleman JB, Woodward M, Lynn MJ, Stulting RD. Risk assessment for ectasia after corneal refractive surgery. *Ophthalmology* 2008;115:37-50.
5. Saad A, Lteif Y, Azan E, Gatinel D. Biomechanical properties of keratoconus suspect eyes. *Invest Ophthalmol Vis Sci* 51:2912-2916.
6. Nilforoushan MR, Speaker M, Marmor M, et al. Comparative evaluation of refractive surgery candidates with Placido topography, Orbscan II, Pentacam, and wavefront analysis. *J Cataract Refract Surg* 2008;34:623-631.
7. Li X, Yang H, Rabinowitz YS. Keratoconus: classification scheme based on videokeratography and clinical signs. *J Cataract Refract Surg* 2009;35:1597-1603.
8. Shirayama-Suzuki M, Amano S, Honda N, Usui T, Yamagami S, Oshika T. Longitudinal analysis of corneal topography in suspected keratoconus. *Br J Ophthalmol* 2009;93:815-819.
9. Rao SN, Raviv T, Majmudar PA, Epstein RJ. Role of Orbscan II in screening keratoconus suspects before refractive corneal surgery. *Ophthalmology* 2002;109:1642-1646.
10. Schweitzer C, Roberts CJ, Mahmoud AM, Colin J, Maurice-Tison S, Kerautret J. Screening of Forme Fruste Keratoconus with the Ocular Response Analyzer. *Invest Ophthalmol Vis Sci* 2009;In Press.
11. Buhren J, Kuhne C, Kohnen T. [Wavefront analysis for the diagnosis of subclinical keratoconus]. *Ophthalmologe* 2006;103:783-790.
12. Buhren J, Kuhne C, Kohnen T. Defining subclinical keratoconus using corneal first-surface higher-order aberrations. *Am J Ophthalmol* 2007;143:381-389.
13. Seiler T, Quurke AW. Iatrogenic keratectasia after LASIK in a case of forme fruste keratoconus. *J Cataract Refract Surg* 1998;24:1007-1009.
14. Schlegel Z, Hoang-Xuan T, Gatinel D. Comparison of and correlation between anterior and posterior corneal elevation maps in normal eyes and keratoconus-suspect eyes. *J Cataract Refract Surg* 2008;34:789-795.
15. Klyce SD. Chasing the suspect: keratoconus. *Br J Ophthalmol* 2009;93:845-847.
16. Klyce SD, Smolek MK, Maeda N. Keratoconus detection with the KISA% method-another view. *J Cataract Refract Surg* 2000;26:472-474.
17. Rabinowitz YS, McDonnell PJ. Computer-assisted corneal topography in keratoconus. *Refract Corneal Surg* 1989;5:400-408.
18. Rabinowitz YS, Nesburn AB, McDonnell PJ. Videokeratography of the fellow eye in unilateral keratoconus. *Ophthalmology* 1993;100:181-186.

19. Rabinowitz YS, Rasheed K. KISA% index: a quantitative videokeratography algorithm embodying minimal topographic criteria for diagnosing keratoconus. *J Cataract Refract Surg* 1999;25:1327-1335.
20. Mahon L, Kent D. Can true monocular keratoconus occur? *Clin Exp Optom* 2004;87:126; author reply 126.
21. Kennedy RH, Bourne WM, Dyer JA. A 48-year clinical and epidemiologic study of keratoconus. *Am J Ophthalmol* 1986;101:267-273.
22. Krachmer JH, Feder RS, Belin MW. Keratoconus and related noninflammatory corneal thinning disorders. *Surv Ophthalmol* 1984;28:293-322.
23. Li X, Rabinowitz YS, Rasheed K, Yang H. Longitudinal study of the normal eyes in unilateral keratoconus patients. *Ophthalmology* 2004;111:440-446.
24. Holland DR, Maeda N, Hannush SB, et al. Unilateral keratoconus. Incidence and quantitative topographic analysis. *Ophthalmology* 1997;104:1409-1413.
25. Ihalainen A. Clinical and epidemiological features of keratoconus genetic and external factors in the pathogenesis of the disease. *Acta Ophthalmol Suppl* 1986;178:1-64.
26. Jacobs DS, Dohlman CH. Is keratoconus genetic? *Int Ophthalmol Clin* 1993;33:249-260.
27. Rabinowitz YS, Maumenee IH, Lundergan MK, et al. Molecular genetic analysis in autosomal dominant keratoconus. *Cornea* 1992;11:302-308.
28. Armitage JA, Bruce AS, Phillips AJ, Lindsay RG. Morphological variants in keratoconus: anatomical observation or aetiologically significant? *Aust N Z J Ophthalmol* 1998;26 Suppl 1:S68-70.
29. Amsler M. [The "forme fruste" of keratoconus.]. *Wien Klin Wochenschr* 1961;73:842-843.
30. Buscemi PM. Nidek corneal navigator software for topographic analysis of corneal states. *J Refract Surg* 2004;20:S747-750.
31. Klyce SD, Karon MD, Smolek MK. Screening patients with the corneal navigator. *J Refract Surg* 2005;21:S617-622.
32. Maeda N, Klyce SD, Smolek MK. Neural network classification of corneal topography. Preliminary demonstration. *Invest Ophthalmol Vis Sci* 1995;36:1327-1335.
33. Ambrosio R, Jr., Alonso RS, Luz A, Coca Velarde LG. Corneal-thickness spatial profile and corneal-volume distribution: tomographic indices to detect keratoconus. *J Cataract Refract Surg* 2006;32:1851-1859.
34. Luz A, Ursulio M, Castaneda D, Ambrosio R, Jr. [Corneal thickness progression from the thinnest point to the limbus: study based on a normal and a keratoconus population to create reference values]. *Arq Bras Oftalmol* 2006;69:579-583.
35. Lim L, Wei RH, Chan WK, Tan DT. Evaluation of keratoconus in Asians: role of Orbscan II and Tomey TMS-2 corneal topography. *Am J Ophthalmol* 2007;143:390-400.
36. Saad A, Gatinel D. Bilateral corneal ectasia after laser in situ keratomileusis in patient with isolated difference in central corneal thickness between eyes. *J Cataract Refract Surg* 36:1033-1035.
37. Pflugfelder SC, Liu Z, Feuer W, Verm A. Corneal thickness indices discriminate between keratoconus and contact lens-induced corneal thinning. *Ophthalmology* 2002;109:2336-2341.

38. Sonmez B, Doan MP, Hamilton DR. Identification of scanning slit-beam topographic parameters important in distinguishing normal from keratoconic corneal morphologic features. *Am J Ophthalmol* 2007;143:401-408.
39. Tanabe T, Tomidokoro A, Samejima T, et al. Corneal regular and irregular astigmatism assessed by Fourier analysis of videokeratography data in normal and pathologic eyes. *Ophthalmology* 2004;111:752-757.
40. Levy D, Hutchings H, Rouland JF, et al. Videokeratographic anomalies in familial keratoconus. *Ophthalmology* 2004;111:867-874.
41. Rabinowitz YS, Rasheed K, Yang H, Elashoff J. Accuracy of ultrasonic pachymetry and videokeratography in detecting keratoconus. *J Cataract Refract Surg* 1998;24:196-201.
42. Auffarth GU, Wang L, Volcker HE. Keratoconus evaluation using the Orbscan Topography System. *J Cataract Refract Surg* 2000;26:222-228.
43. Tomidokoro A, Oshika T, Amano S, Higaki S, Maeda N, Miyata K. Changes in anterior and posterior corneal curvatures in keratoconus. *Ophthalmology* 2000;107:1328-1332.
44. Rabinowitz YS. Keratoconus. *Surv Ophthalmol* 1998;42:297-319.